

The pion light-cone distribution amplitude from the pion electromagnetic form factor

Shan Cheng^a, Alexander Khodjamirian^b, and Aleksey V. Rusov^c

^a*School of Physics and Electronics, Hunan University,
410082 Changsha, China*

^b*Theoretische Physik 1, Naturwissenschaftlich-Technische Fakultät,
Universität Siegen, D-57068 Siegen, Germany*

^c*Institute for Particle Physics Phenomenology, Durham University,
DH1 3LE Durham, United Kingdom*

Abstract

We suggest to probe the pion light-cone distribution amplitude, applying a dispersion relation for the pion electromagnetic form factor. Instead of the standard dispersion relation, we use the equation between the spacelike form factor $F_\pi(Q^2)$ and the integrated modulus of the timelike form factor. For $F_\pi(Q^2)$, the QCD light-cone sum rule with a dominant twist-2 term is used. Adopting for the pion twist-2 distribution amplitude a certain combination of the first few Gegenbauer polynomials, it is possible to fit their coefficients $a_{2,4,6,\dots}$ (Gegenbauer moments) from this equation, employing the measured pion timelike form factor. For the exploratory fit we use the data of the BaBar collaboration. The results definitely exclude the asymptotic twist-2 distribution amplitude. Also the model with a single $a_2 \neq 0$ is disfavoured by the fit. Considering the models with $a_{n>2} \neq 0$, we find that the fitted values of the second and fourth Gegenbauer moments cover the intervals $a_2(1\text{GeV}) = (0.22 - 0.33)$, $a_4(1\text{GeV}) = (0.12 - 0.25)$. The higher moments starting from a_8 are consistent with zero, albeit with large uncertainties. The spacelike pion form factor obtained in two different ways, from the dispersion relation and from the light-cone sum rule, agrees, within uncertainties, with the measurement by the Jefferson Lab F_π collaboration.

1 Introduction

The light-cone distribution amplitudes (DAs) are the key elements in several QCD methods used to describe the hard exclusive scattering and heavy hadron decays. For the processes involving a pion, the accuracy of this description depends first of all on our knowledge of the leading twist-2 pion DA. The expansion of this DA in orthogonal Gegenbauer polynomials reduces the necessary input to their coefficients a_n ($n = 2, 4, 6, \dots$) known as the Gegenbauer moments. In many practical applications only the low moments are retained in the pion twist-2 DA. Such a parametrization is justified by the fact that the anomalous dimension of the multiplicatively renormalizable moment a_n grows with the number n , so that the contributions of higher moments to the processes with a large momentum scale are suppressed. Hence, for an accurate description of the pion DA, the knowledge of the first few Gegenbauer moments at a certain normalization scale is of utmost importance.

In QCD, the Gegenbauer moments are related to the vacuum-to-pion matrix elements of the local quark-antiquark operators with polynomial combinations of derivatives acting on the quark field. Needless to say, these moments are genuinely nonperturbative objects. Currently, only the second Gegenbauer moment a_2 is accessible in the lattice QCD. Recently, it was obtained in Ref. [1] with an unprecedented accuracy (for earlier results see Ref. [2,3]). The moments with $n > 2$ are not accessible with these lattice computations, because of the growing number of derivatives in the underlying quark-antiquark operators. Alternative lattice QCD techniques [4,5] avoiding this problem are being developed.

The method of QCD sum rules [6] based on the two-point correlation function was pioneered for the calculation of Gegenbauer moments in Ref. [7] and further used, e.g. in Refs. [8,9]. This method is also limited to the lowest moment a_2 . Extension to higher moments is possible if a nonlocal vacuum condensate is introduced and modeled [10,11]. A different approach employs the pion form factors obtained from the QCD light-cone sum rules (LCSRs). Initiated in Refs. [12,13], this technique enables to calculate both the hard-scattering and soft-overlap contributions to the pion electromagnetic (e.m.) form factor [14,15] or to the photon-pion transition form factor [16,17] at large spacelike momentum transfers, practically at $|q^2| \gtrsim 1 \text{ GeV}^2$. The calculation is based on the light-cone expansion of a vacuum-to-pion correlation function in terms of the pion DAs of growing twist. For both form factors, the dominant part of the sum rule contains the twist-2 DA convoluted with a calculable function. This opens up a possibility to estimate or at least to constrain the Gegenbauer moments, comparing the LCSR result for a form factor with its measurement in the spacelike region. For the photon-pion transition form factor this analysis was done employing several available measurements of the $\gamma^*\gamma \rightarrow \pi^0$ process (see e.g. Ref. [17,18]).

In this paper, we concentrate on the pion e.m. form factor denoted as $F_\pi(q^2)$. It is possible to estimate the Gegenbauer moments, assuming a certain ansatz for the pion DA and fitting the resulting LCSR for the spacelike form factor $F_\pi(q^2 < 0)$ to its measured values. The most accurate measurements to date have been performed at Jefferson Lab [20] extracting the form factor from the cross section of the pion electroproduction on a nucleon target. An earlier estimate of a_2 and a_4 fitting the LCSR to these data was obtained in Ref. [21] (see also Refs. [22,23]). However, the Jefferson Lab measurements are limited to relatively small momentum transfers, $|q^2| \lesssim 2.5 \text{ GeV}^2$ and depend on the model description of the intermediate pion coupled to the nucleon¹.

¹Note that a direct measurement of the pion spacelike e.m. form factor via the electron-pion scattering

The pion e.m. form factor $F_\pi(s)$ in the timelike region $q^2 = s > 4m_\pi^2$ is directly accessible measuring the $e^+e^- \rightarrow \pi^+\pi^-$ cross section at a given c.m. energy \sqrt{s} of the e^+e^- collision. In addition to the ρ -resonance domain, $s \lesssim 1.0 \text{ GeV}^2$, which was scanned in great detail in several experiments, quite accurate data [25] were obtained at larger energies, up to $s \simeq 9.0 \text{ GeV}^2$, by the BaBar collaboration, with the help of the initial-state radiation technique. One also has to mention the data of Belle collaboration [26] on the related (via isospin symmetry) pion weak vector form factor in the $\tau \rightarrow \pi\pi\nu_\tau$ decay.

The purpose of this paper is to demonstrate that the timelike form factor $F_\pi(s)$ can provide an additional information about the pion DAs. This is achieved by combining the dispersion relation for the timelike form factor with the LCSR for the spacelike form factor. Note however that the standard dispersion relation demands the knowledge of the form factor imaginary part which is not directly measured and depends on the parametrization of $F_\pi(s)$. To avoid the uncertainty induced by the restoration of the imaginary part from the measured modulus of the timelike form factor, we suggest to use a modified dispersion relation in which the spacelike form factor is equal to the integral over $|F_\pi(s)|^2$. One crucial condition for the validity of this relation is the (phenomenologically justified) assumption that the form factor $F_\pi(q^2)$ does not possess zeros in the complex plane of the variable q^2 .

In what follows, in Section 2 we derive and discuss in detail the modified dispersion relation used in our analysis. In Section 3 we present the necessary ingredients of the LCSR for the spacelike pion e.m. form factor. Section 4 contains the description of the timelike form factor data. In Section 5 the details of the form factor fit to the dispersion integral and the resulting estimates of Gegenbauer moments are presented, and Section 6 contains our conclusions.

2 Dispersion relations for the pion form factor

We use the standard definition of the pion e.m. form factor in the spacelike region:

$$\langle \pi^+(p_2) | j_\mu^{em} | \pi^+(p_1) \rangle = (p_1 + p_2)_\mu F_\pi(q^2), \quad (1)$$

where $j_\mu^{em} = (1/2)(\bar{u}\gamma_\mu u - \bar{d}\gamma_\mu d)$ is the isovector component of the quark e.m. current, and $q = p_2 - p_1$ is the momentum transfer. The form factor obeys the normalization condition $F_\pi(0) = 1$, reflecting the unit electric charge of π^+ . The standard dispersion relation

$$F_\pi(q^2) = \frac{1}{\pi} \int_{s_0}^{\infty} ds \frac{\text{Im}F_\pi(s)}{s - q^2 - i\epsilon}, \quad (2)$$

connects the spacelike pion form factor $F_\pi(q^2)$ at $q^2 < 0$ with the imaginary part of the timelike form factor $F_\pi(s)$ integrated over s above the two-pion threshold $s_0 \equiv 4m_\pi^2$. Note that subtractions are not necessary in Eq. (2) due to the power asymptotics of the pion form factor predicted in QCD [27–30]:

$$F_\pi(q^2) \sim \frac{1}{q^2} \quad \text{at } |q^2| \rightarrow \infty. \quad (3)$$

In order to obtain the spacelike form factor $F_\pi(q^2 < 0)$ from the dispersion relation (2), one has to extract the imaginary part of the timelike form factor from its modulus squared

exists [24], but only at very small momentum transfers, that is, in the region where LCSR is not applicable.

$|F_\pi(s)|^2$ measured in $e^+e^- \rightarrow \pi^+\pi^-$. This extraction demands a realistic parameterization of $F_\pi(s)$, which satisfies the hadronic unitarity relation and reflects the presence of the ρ -resonance and its radial excitations in the P -wave channel of the pion-pion scattering. Examples of elaborated parameterizations can be found e.g., in Refs. [31–34]. Expressing $F_\pi(s)$ in terms of certain parameters, one has to fit them, comparing the resulting $|F_\pi(s)|^2$ to its measured values. Reconstructing $\text{Im}F_\pi(s)$ in this indirect way, one eventually introduces additional uncertainties.

In this work, we suggest to use an alternative dispersion relation directly expressing the spacelike form factor via the integral over the modulus of the timelike form factor. In the literature, this relation is called *the modulus representation* and goes back to Ref. [35]. To derive it, we introduce the following auxiliary function:

$$g_\pi(q^2) \equiv \frac{\ln F_\pi(q^2)}{q^2 \sqrt{s_0 - q^2}}. \quad (4)$$

This function has no singularities in the complex plane of the variable q^2 , apart from the region $q^2 = s > s_0$ on the real axis. This statement is only valid under the assumption that the form factor $F_\pi(q^2)$ is free from zeros in the complex q^2 plane², so that the logarithm in Eq. (4) does not diverge at any q^2 . Note also that $g_\pi(0)$ is finite, as follows from the normalization of the pion form factor at $q^2 = 0$. Furthermore, since $F_\pi(q^2)$ has a power asymptotics, the numerator in Eq. (4) has a logarithmic behaviour. Therefore,

$$g_\pi(q^2) \sim \frac{1}{(q^2)^\alpha} \quad \text{at } |q^2| \rightarrow \infty, \quad (5)$$

where $\alpha > 1$. This condition enables a dispersion relation for the function $g_\pi(q^2)$ which is derived in the same way as for the form factor. We start from the Cauchy theorem:

$$g_\pi(q^2) = \frac{1}{2\pi i} \int_C dz \frac{g_\pi(z)}{z - q^2}, \quad (6)$$

where the integration contour C circumvents the singularities on the real axis at $s > s_0$. This contour consists of the two straight lines connected by a large circle with the radius R and by a semicircle with an infinitesimal radius $\epsilon \rightarrow 0$, centered at $s = s_0$. After that, we discard the integral over the circle at $R \rightarrow \infty$, making use of the asymptotics (5). The integral over the semicircle vanishes at $\epsilon \rightarrow 0$. We also use the fact that the function $g_\pi(s)$ is real valued at $s < s_0$ on the real axis and apply the Schwartz reflection principle:

$$g_\pi(s + i\epsilon) - g_\pi(s - i\epsilon) = 2i \text{Im } g_\pi(s), \quad \epsilon \rightarrow 0.$$

Finally, we are left with the relation

$$g_\pi(q^2) = \frac{1}{\pi} \int_{s_0}^{\infty} ds \frac{\text{Im } g_\pi(s)}{s - q^2 - i\epsilon}. \quad (7)$$

On the real axis, at $s > s_0$, the singularities of the function $g_\pi(s)$ are determined by an overlap of the “dynamical” poles and branch points contributing to $\text{Im}F_\pi(s)$ with the imaginary part

²The arguments in favour of this conjecture can be found in Ref. [36], a more recent discussion of form factor zeros including relevant references can be found in Ref. [37].

of the square root function $\sqrt{s_0 - s}$ which has a branch point at $s = s_0$. Note that, due to our standard choice of $i\epsilon$ in the dispersion relation ³,

$$\sqrt{s_0 - (s + i\epsilon)}\Big|_{\epsilon \rightarrow 0} = -i\sqrt{s - s_0}, \quad s > s_0. \quad (8)$$

Representing

$$F_\pi(s) = |F_\pi(s)|e^{i\delta_\pi(s)}$$

and using Eq. (8), we obtain, at $s > s_0$,

$$\text{Im } g_\pi(s) = \text{Im} \left[\frac{\ln(|F_\pi(s)|e^{i\delta_\pi(s)})}{-is\sqrt{s - s_0}} \right] = \frac{1}{s\sqrt{s - s_0}} \text{Im} \left[\frac{\ln |F_\pi(s)| + i\delta_\pi(s)}{-i} \right] = \frac{\ln |F_\pi(s)|}{s\sqrt{s - s_0}}. \quad (9)$$

Finally, substituting this function in Eq. (7), we arrive at

$$\frac{\ln F_\pi(q^2)}{q^2\sqrt{s_0 - q^2}} = \frac{1}{2\pi} \int_{s_0}^{\infty} \frac{ds \ln |F_\pi(s)|^2}{s\sqrt{s - s_0}(s - q^2)}, \quad q^2 < s_0, \quad (10)$$

or, equivalently,

$$F_\pi(q^2) = \exp \left[\frac{q^2\sqrt{s_0 - q^2}}{2\pi} \int_{s_0}^{\infty} \frac{ds \ln |F_\pi(s)|^2}{s\sqrt{s - s_0}(s - q^2)} \right], \quad q^2 < s_0. \quad (11)$$

The above equation represents the modified dispersion relation we are aiming at. This formula was suggested and used in Ref. [35]; other applications and modifications can be found e.g., in Refs. [36–38]. Note that Eq. (11) automatically ensures that $F_\pi(0) = 1$. As demonstrated in Ref. [35], if, hypothetically, the form factor possesses zeros in the complex q^2 plane, then, instead of the relation (11), $F_\pi(q^2 < 0)$ obeys narrow upper and lower bounds that are again determined by the modulus of the timelike form factor. This case deserves a separate analysis which remains beyond the scope of this paper.

3 LCSR for the spacelike pion form factor

The LCSR for the pion e.m. form factor is derived from the correlation function:

$$\begin{aligned} \mathcal{F}_{\rho\mu}(p, q) &= i \int d^4x e^{iqx} \langle 0 | T \{ \bar{d}(0) \gamma_\rho \gamma_5 u(0) j_\mu^{\text{em}}(x) \} | \pi^+(p) \rangle \\ &= ip_\rho p_\mu \mathcal{F}((p - q)^2, Q^2) + \dots, \end{aligned} \quad (12)$$

where only the relevant Lorentz structure is shown, and the others are indicated by the ellipsis. The invariant amplitude depends on the two kinematical variables $(p - q)^2$ and $Q^2 = -q^2$ and obeys a hadronic dispersion relation in the variable $(p - q)^2$ at fixed Q^2 :

$$\mathcal{F}((p - q)^2, Q^2) = \frac{2f_\pi F_\pi(Q^2)}{m_\pi^2 - (p - q)^2} + \int_{(3m_\pi)^2}^{\infty} ds \frac{\rho^h(s, Q^2)}{s - (p - q)^2}, \quad (13)$$

³As one can see below, the other branch with the $+i$ multiplying the square root would lead to an unphysical divergence of the pion form factor, $\lim_{q^2 \rightarrow -\infty} F_\pi(q^2) = \infty$.

where the lowest pole corresponds to the intermediate one-pion state interpolated by the axial-vector current. The residue of the pion pole contains a product of the pion decay constant and the form factor we are interested in. The integral over heavier states with the quantum numbers of the pion or a_1 meson will be approximated using the quark-hadron duality. Note that the lightest continuum state in this channel consists of three pions.

In the correlation function (12), at large Q^2 and $|(p-q)^2|$, the product of the axial-vector and e.m. currents is expanded near the light-cone $x^2 \simeq 0$ in a series of nonlocal operators. Their pion-to-vacuum matrix elements generate contributions of the pion DAs with growing twists $t = 2, 4, 6$ ⁴.

The leading twist-2 term of the light-cone operator-product expansion (OPE) contains the pion twist-2 DA which is defined in a standard way:

$$\langle 0 | \bar{d}(0) \gamma_\mu \gamma_5 u(x) | \pi^+(p) \rangle = i p_\mu f_\pi \int_0^1 du e^{-iupx} \varphi_\pi(u, \mu), \quad (14)$$

where μ is the scale determined by the characteristic light-cone separation $\mu \sim 1/\sqrt{|x^2|}$. The standard expansion of the pion DA in Gegenbauer polynomials will be used in the following form:

$$\varphi_\pi(u, \mu) = 6u\bar{u} \left(1 + \sum_{n=2,4,\dots} a_n(\mu_0) L_n(\mu, \mu_0) C_n^{(3/2)}(u - \bar{u}) \right), \quad (15)$$

where $\bar{u} = 1 - u$. The multiplicative renormalization from the default scale μ_0 to the variable scale μ is taken into account at LO by the logarithmic factor

$$L_n(\mu, \mu_0) = \left[\frac{\alpha_s(\mu)}{\alpha_s(\mu_0)} \right]^{\gamma_n^{(0)}/\beta_0} \quad (16)$$

with the anomalous dimensions given by

$$\gamma_n^{(0)} = 4C_F \left(\psi(n+2) + \gamma_E - \frac{3}{4} - \frac{1}{2(n+1)(n+2)} \right), \quad (17)$$

where $\psi(n)$ is the digamma function and $\beta_0 = 11 - 2/3n_f$ is the QCD beta-function. Since at $\mu \rightarrow \infty$ all $L_n(\mu, \mu_0) \rightarrow 0$, the first term in Eq. (14) determines the asymptotic shape of the DA.

The correlation function (12) obtained in Ref. [15] (see also Ref. [22]) includes the twist-2 part consisting of the leading order (LO) term and the next-to-leading order (NLO), $O(\alpha_s)$ radiative corrections. In addition, the subleading twist-4 term at LO and the twist-6 term in the factorizable approximation are taken into account. Leaving aside many details, we present the LO twist-2 part of the invariant amplitude in Eq. (12):

$$\begin{aligned} \mathcal{F}^{(\text{tw}2, \text{LO})}((p-q)^2, Q^2) &= 2f_\pi \int_0^1 du \frac{u \varphi_\pi(u)}{\bar{u}Q^2 - u(p-q)^2} \\ &= \int_0^\infty \frac{ds}{s - (p-q)^2} \left[2f_\pi \frac{Q^2}{(Q^2 + s)^2} \varphi_\pi(u(s)) \right]. \end{aligned} \quad (18)$$

⁴Note that in the chiral symmetry limit adopted here the contributions of odd twists $t = 3, 5$ vanish.

The second equation in the above, obtained by transforming the integration variable: $u = Q^2/(s + Q^2)$, has a form of dispersion relation allowing us to interpret the expression in the square brackets as the OPE spectral density. According to the quark-hadron duality prescription, the integral over $\rho^h(s, Q^2)$ in Eq. (13) is replaced by the one in the second line of Eq. (18), with the lower limit equal to the effective duality threshold s_0^π . Equating the two different representations of the correlation function, Eqs. (13) and (18), subtracting the dual parts from both sides, performing the Borel transformation and transforming back to the variable u , we reproduce the LCSR for the form factor in the LO, twist-2 approximation:

$$F_\pi^{(\text{tw}2, \text{LO})}(Q^2) = \int_{u_0^\pi}^1 du \varphi_\pi(u, \mu) \exp\left(-\frac{\bar{u} Q^2}{u M^2}\right), \quad (19)$$

where $u_0^\pi = Q^2/(s_0^\pi + Q^2)$. The complete LCSR for the pion e.m. form factor obtained in Refs. [15, 22] can be presented in a compact form:

$$F_\pi^{(\text{LCSR})}(Q^2) = F_\pi^{(\text{tw}2, \text{LO})}(Q^2) + F_\pi^{(\text{tw}2, \text{NLO})}(Q^2) + F_\pi^{(\text{tw}4, \text{LO})}(Q^2) + F_\pi^{(\text{tw}6, \text{fact})}(Q^2), \quad (20)$$

where the second after Eq. (19) important contribution is the NLO twist-2 term. It has a factorized form with respect to the pion DA:

$$F_\pi^{(\text{tw}2, \text{NLO})}(Q^2) = \frac{\alpha_s C_F}{4\pi} \left[\int_{u_0^\pi}^1 du \varphi_\pi(u, \mu) \mathcal{F}_{\text{soft}}(u, \mu, M^2, s_0^\pi) + \int_0^{u_0^\pi} du \varphi_\pi(u, \mu) \mathcal{F}_{\text{hard}}(u, \mu, M^2, s_0^\pi) \right], \quad (21)$$

where the analytical expressions for the functions $\mathcal{F}_{\text{soft}}$ and $\mathcal{F}_{\text{hard}}$ are given in Ref. [15]. Note that, the first (second) term in the above equation can be interpreted as the radiative correction to the soft-overlap part (19) (as the hard-scattering part) of the form factor.

We substitute the expansion (15) in Eqs. (19) and (21) and represent the LCSR (20) in a form containing a linear combination of Gegenbauer moments normalized at the default scale μ_0 :

$$F_\pi^{(\text{LCSR})}(Q^2) = F_\pi^{(\text{tw}2, \text{as})}(Q^2) + \sum_{n=2,4,\dots} a_n(\mu_0) f_n(Q^2, \mu, \mu_0) + F_\pi^{(\text{tw}4, \text{LO})}(Q^2) + F_\pi^{(\text{tw}6, \text{fact})}(Q^2), \quad (22)$$

where the coefficient functions

$$\begin{aligned} f_n(Q^2, \mu, \mu_0) = & 6 L_n(\mu, \mu_0) \left\{ \int_{u_0^\pi}^1 du u \bar{u} C_n^{(3/2)}(u - \bar{u}) e^{-\bar{u} Q^2/(u M^2)} \right. \\ & + \frac{\alpha_s C_F}{4\pi} \left[\int_{u_0^\pi}^1 du u \bar{u} C_n^{(3/2)}(u - \bar{u}) \mathcal{F}_{\text{soft}}(u, \mu, M^2, s_0^\pi) \right. \\ & \left. \left. + \int_0^{u_0^\pi} du u \bar{u} C_n^{(3/2)}(u - \bar{u}) \mathcal{F}_{\text{hard}}(u, \mu, M^2, s_0^\pi) \right] \right\} \quad (23) \end{aligned}$$

include the NLO corrections. The dominant part of the LCSR (22), describing the twist-2 contribution with the asymptotic DA, is reduced [15] to a compact expression

$$F_{\pi}^{(\text{tw}2, \text{as})}(Q^2) = 6 \int_0^{s_0^{\pi}} ds e^{-s/M^2} \frac{s Q^4}{(s + Q^2)^4} \left\{ 1 + \frac{\alpha_s C_F}{4\pi} \left[\frac{\pi^2}{3} - 6 - \ln^2 \frac{Q^2}{s} + \frac{s}{Q^2} + \frac{Q^2}{s} \right] \right\} \quad (24)$$

which is, as expected, independent of the factorization scale μ . Importantly, apart from the soft-overlap contribution decreasing as $\sim 1/Q^4$, the expression in Eq. (24) also reproduces the asymptotic regime:

$$\lim_{Q^2 \rightarrow \infty} F_{\pi}^{(\text{tw}2, \text{as})}(Q^2) = \frac{8\pi\alpha_s f_{\pi}^2}{Q^2} \quad (25)$$

which coincides with the perturbative QCD factorization formula [27–30] for the asymptotic pion DAs. As shown in Ref. [15], Eq. (25) follows from the $Q^2 \rightarrow \infty$ limit of Eq. (24), if we use the conventional QCD sum rule [6] for the square of the pion decay constant,

$$f_{\pi}^2 = \frac{1}{4\pi^2} \int_0^{s_0^{\pi}} ds e^{-s/M^2} + \dots,$$

where the radiative corrections and condensate terms contain an extra α_s and are absent in our approximation. Importantly, at moderate Q^2 the soft-overlap contribution dominates in the form factor (22).

For the twist-4 contribution to the LCSR (22) we use the updated result from Ref. [22] obtained assuming the asymptotic form of all twist-4 DAs entering this contribution:

$$F_{\pi}^{(\text{tw}4, \text{LO})}(Q^2) = \frac{40}{3} \delta_{\pi}^2(\mu) \int_0^{s_0^{\pi}} ds e^{-s/M^2} \frac{Q^8}{(Q^2 + s)^6} \left(1 - \frac{9s}{Q^2} + \frac{9s^2}{Q^4} - \frac{s^3}{Q^6} \right), \quad (26)$$

where $\delta_{\pi}^2(\mu)$ denotes the normalization parameter of the twist-4 pion DAs describing the vacuum-to-pion matrix element of the quark-antiquark-gluon operator

$$\langle 0 | \bar{d} \tilde{G}_{\nu\mu} \gamma^{\nu} u | \pi^{+}(p) \rangle = -i \delta_{\pi}^2 f_{\pi} p_{\mu}. \quad (27)$$

We also have checked that adding the nonasymptotic terms [9] to the twist-4 DAs has a negligible numerical impact on the value given by Eq. (26).

Finally, for the twist-6 term contribution to the form factor we use the factorization approximation, reduced [15] to the expression depending on the quark condensate density:

$$F_{\pi}^{(\text{tw}6, \text{fact})}(Q^2) = \frac{4\pi\alpha_s C_F}{3f_{\pi}^2 Q^4} \langle \bar{q}q \rangle^2. \quad (28)$$

It is convenient to represent the complete LCSR (22) for the spacelike form factor in a more compact form:

$$F_{\pi}^{(\text{LCSR})}(Q^2) = F_{\pi}^{(\text{as})}(Q^2) + \sum_{n=2,4,..} a_n(\mu_0) f_n(Q^2, \mu, \mu_0), \quad (29)$$

where we use the notation

$$F_{\pi}^{(\text{as})}(Q^2) = F_{\pi}^{(\text{tw2,as})}(Q^2) + F_{\pi}^{(\text{tw4,LO})}(Q^2) + F_{\pi}^{(\text{tw6,fact})}(Q^2)$$

and separate the part containing the asymptotic DA from the contribution generated by nonasymptotic terms in the Gegenbauer expansion. Below, this expression will be used in the l.h.s of the dispersion representation (11). Eq. (29) is valid in the spacelike region, practically at $Q^2 = -q^2 \gtrsim 1.0 \text{ GeV}^2$. We also constrain the momentum transfer from above taking $Q^2 \lesssim 10 \text{ GeV}^2$. The reasons are twofold. Firstly, as analysed in Ref. [15], the missing higher-order (NNLO) perturbative corrections as well as the double logarithmic $\sim \ln^2 Q^2$ terms reminiscent of the Sudakov logarithms (such a term is already present in Eq. (24)) may become numerically important in LCSR at very large Q^2 . Secondly, as we checked numerically, at Q^2 above the adopted upper limit the dispersion integral in Eq. (11) becomes more sensitive to the timelike form factor above the region where it is measured (see the next section).

Another important limitation concerns the Borel parameter and is common for all QCD sum rules. The truncation of OPE on one hand and the validity of the duality approximation on the other hand demand that this parameter lies within a certain interval, typically in the ballpark of $M^2 = 1.0 \text{ GeV}^2$. Varying this and other input parameters entering Eq. (29) we estimate the uncertainty of the spacelike form factor obtained from LCSR.

4 Pion form factor in the timelike region

Our remaining task is to specify the modulus of the timelike pion form factor entering r.h.s. of the relation (11). To this end we use the rich data set on the $e^+e^- \rightarrow \pi^+\pi^-(\gamma)$ cross section measured in the range

$$0.305 \text{ GeV} < \sqrt{s} < 2.95 \text{ GeV}$$

by the BaBar collaboration [25]. We denote by $s_{\text{max}} \simeq 8.70 \text{ GeV}^2$ the upper boundary of this range and split the integration region in Eq. (11) into two intervals so that:

$$|F_{\pi}(s)| = \Theta(s_{\text{max}} - s) |F_{\pi}^{(\text{data})}(s)| + \Theta(s - s_{\text{max}}) |F_{\pi}^{(\text{tail})}(s)|. \quad (30)$$

The pion form factor extracted from the BaBar data in Ref. [25] was fitted to a superposition of four ρ resonances, starting from $\rho(770)$, including the three subsequent radial excitations and taking into account the $\rho - \omega$ mixing:

$$F_{\pi}^{(\text{data})}(s) = \frac{1}{1 + c_{\rho'} + c_{\rho''} + c_{\rho'''}} \left[\text{BW}_{\rho}^{\text{GS}}(s, m_{\rho}, \Gamma_{\rho}) \frac{1 + c_{\omega} \text{BW}_{\omega}^{\text{KS}}(s, m_{\omega}, \Gamma_{\omega})}{1 + c_{\omega}} \right. \\ \left. + c_{\rho'} \text{BW}_{\rho'}^{\text{GS}}(s, m_{\rho'}, \Gamma_{\rho'}) + c_{\rho''} \text{BW}_{\rho''}^{\text{GS}}(s, m_{\rho''}, \Gamma_{\rho''}) + c_{\rho'''} \text{BW}_{\rho'''}^{\text{GS}}(s, m_{\rho'''}, \Gamma_{\rho'''}) \right]. \quad (31)$$

In this expression, all ρ resonances (the ω resonance) are described by the Gounaris-Sakurai (GS) representation [41] (the Kühn-Santamaria (KS) representation [42]) of the Breit-Wigner function. In all ρ -resonance terms in Eq. (31), the dependence of the width on the energy is taken into account and, by construction, the normalization condition $F_{\pi}(0) = 1$ is valid.

R	m_R (MeV)	Γ_R (MeV)	$ c_R $	ϕ_R (rad)
ρ	775.02 ± 0.35	149.59 ± 0.67	1.0	0
ω	781.91 ± 0.24	8.13 ± 0.45	$(1.644 \pm 0.061) \times 10^{-3}$	-0.011 ± 0.037
ρ'	1493 ± 15	427 ± 31	0.158 ± 0.018	3.76 ± 0.10
ρ''	1861 ± 17	316 ± 26	0.068 ± 0.009	1.39 ± 0.20
ρ'''	2254 ± 22	109 ± 76	$0.0051^{+0.0034}_{-0.0019}$	0.70 ± 0.51

Table 1: Parameters of the resonances $R = \rho, \omega, \rho', \rho'', \rho'''$ in Eq. (31), obtained in Ref. [25] from the fit to the data on the timelike pion form factor. The errors are added in quadrature.

For convenience, in the Appendix we present the definitions of the BW function used in Eq. (31). The numerical values of the fit parameters of resonances are taken from Ref. [25] and shown in Table 1. Note that the fit returns complex valued coefficients multiplying the BW functions:

$$c_R = |c_R|e^{i\phi_R}, \quad R = \omega, \rho', \rho'', \rho''',$$

implicitly reflecting a certain mixing between resonance contributions. The timelike pion form factor measured by the BaBar collaboration is shown in Fig. 1.

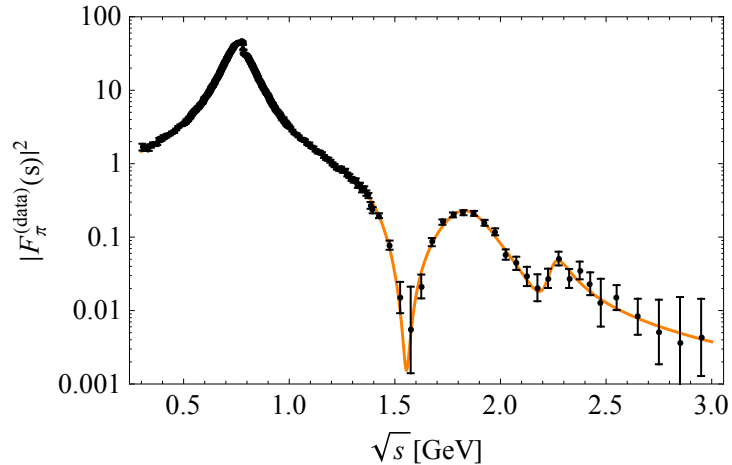


Figure 1: The pion timelike form factor squared measured by the BaBar collaboration [25]. The dots with error bars are the data points and the orange curve is the fit of the data to the resonance model (31).

Since we are only interested in the integral over $|F_\pi(s)|$, the expression in Eq. (31) is merely treated as a fit function for the data points below s_{\max} . Moreover, this formula is not sufficiently accurate to describe the timelike form factor at $s > s_{\max}$ for the following reasons. Firstly, the hadronic states above the first four ρ resonances are not taken into account, and, secondly, as we have checked numerically, the form factor described by Eq. (31) deviates from the asymptotic behaviour $F_\pi(s) \sim 1/s$ at very large s . Hence, being continued to large negative $s = q^2 \rightarrow -\infty$ it does not satisfy the asymptotic QCD regime (25), which is also obeyed by the LCSR. Therefore, for the high-energy part of the integrand in Eq. (11) denoted as $F^{(\text{tail})}(s)$ in Eq. (30), we prefer to use a theory-motivated representation of the pion form factor which supersedes the four-resonance formula (31).

As such, we adopt the form factor suggested in Ref. [39] (see also Ref. [40]) and inspired by the dual-resonance models and $N_c = \infty$ limit of QCD. The main assumption is to replace the spectrum of hadronic states contributing to the pion form factor by an infinite set of equidistant ρ resonances:

$$F_\pi^{(N_c=\infty)}(s) = \sum_{n=0}^{\infty} c_n \text{BW}_n(s). \quad (32)$$

Each resonance contribution enters the sum in a simple Breit-Wigner form

$$\text{BW}_n(s) = \frac{m_n^2}{m_n^2 - s - im_n\Gamma_n}, \quad (33)$$

with a weighting coefficient:

$$c_n = \frac{(-1)^n \Gamma(\beta - 1/2)}{\alpha' m_n^2 \sqrt{\pi} \Gamma(n+1) \Gamma(\beta - 1 - n)}. \quad (34)$$

In the above, the parameter $\alpha' = 1/2m_\rho^2$ is related to the ρ -meson Regge trajectory, and the masses of equidistant resonances are

$$m_n^2 = m_\rho^2(1 + 2n).$$

In addition, in this model the total widths are assumed to grow linearly with the resonance mass:

$$\Gamma_n = \gamma m_n, \quad (35)$$

and the parameter $\gamma = 0.193$ is adjusted to the total width of $\rho(770)$. Assuming that

$$F_\pi^{(\text{tail})}(s) = F_\pi^{(N_c=\infty)}(s), \quad s \geq s_{\text{max}}, \quad (36)$$

we fix the remaining parameter β in Eq. (34) by imposing the matching condition:

$$|F_\pi^{(\text{data})}(s_{\text{max}})| = |F_\pi^{(\text{tail})}(s_{\text{max}})|, \quad (37)$$

from which we have fitted

$$\beta = 2.09 \pm 0.13. \quad (38)$$

In the numerical analysis, we use Eq. (32) retaining a finite sum with 100 resonance terms; we checked that increasing this number does not produce visible changes in the integral (11).

The advantage of the model (32) is that it effectively includes all hadronic states contributing to the form factor. In particular, the resonance widths partially account for the continuum of intermediate hadronic states coupled to the resonances (see Ref. [40] for details). Moreover, if one introduces the correct threshold behavior, so that at all $\Gamma_n = 0$ at $s < s_0 = 4m_\pi^2$, then Eq. (32) with vanishing widths is reduced to the Euler Beta function. It correctly reproduces the normalization $F_\pi^{(N_c=\infty)}(0) = 1$ and reveals the asymptotic behaviour

$$\lim_{s \rightarrow -\infty} F_\pi^{(N_c=\infty)}(s) \sim 1/s^{\beta-1},$$

which, having in mind the estimate (38), is close to the QCD asymptotics.

One has to admit that the model (32) does not provide a sufficiently accurate description of the timelike form factor in the region below s_{max} where the overlapping pattern of the

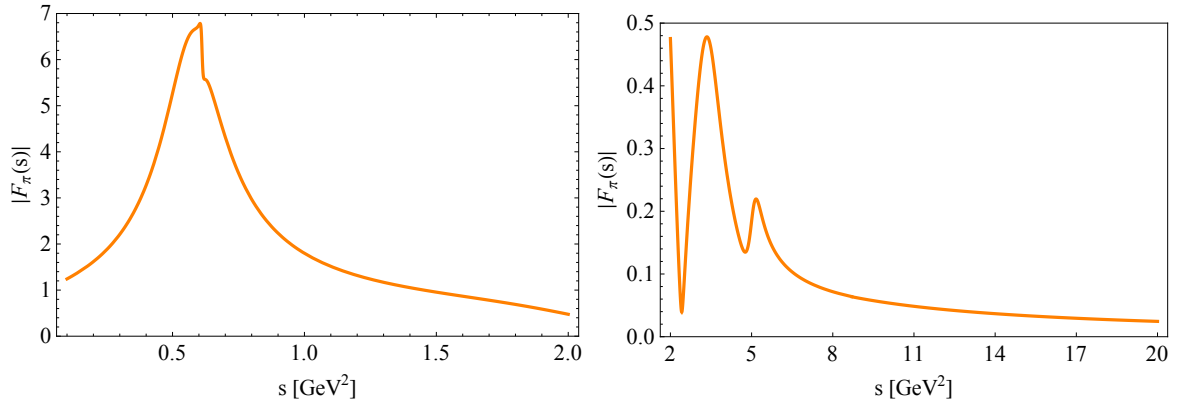


Figure 2: The modulus of the pion timelike form factor as defined in Eq. (30).

lowest ρ resonances deserves a more detailed description, and a small but visible admixture of ω has to be taken into account (see Table 1 [25]). In Ref. [40] the $N_c = \infty$ model was modified by replacing the contributions of the first few resonances with GS or KS resonance formulas. However, we do not need such an improvement here because the form factor $F_\pi^{(N_c=\infty)}(s)$ is used only in the region of large s . In Fig. 2 the modulus of the timelike pion form factor resulting from Eq. (30) is plotted where Eqs. (31) and (36) are used.

Our final comment concerns the conventional dispersion relation (2), which we also have probed, numerically calculating the imaginary part of the timelike form factor from Eq. (30). The resulting form factor at $q^2 < 0$ is very close to the one obtained with the modulus representation. The difference varies between $\approx 1\%$ for $q^2 = -1.0 \text{ GeV}^2$ and $\approx 4\%$ at $q^2 = -10.0 \text{ GeV}^2$. This comparison may indicate that the zeros of the pion e.m. form factor are either absent or their influence is beyond the accuracy of our analysis.

5 Estimates of the Gegenbauer moments

Turning to the numerical analysis, our main task is to fit the Gegenbauer moments from the relation (11) rewritten as:

$$F_\pi^{(\text{LCSR})}(Q^2) = \exp \left[\frac{-Q^2 \sqrt{s_0 + Q^2}}{2\pi} \int_{s_0}^{\infty} \frac{ds \ln |F_\pi(s)|^2}{s \sqrt{s - s_0} (s + Q^2)} \right], \quad (39)$$

where the l.h.s is given by Eq. (29) and the integrand on r.h.s. by Eq. (30). To specify the parameters of the LCSR, following Ref. [15], we adopt for DAs a variable normalization scale:

$$\mu^2 = (1 - u)Q^2 + uM^2. \quad (40)$$

This choice takes into account that a typical factorization scale in the correlation function is determined by the interplay of two external variables Q^2 and $|(p - q)^2|$, the latter being effectively replaced by the Borel parameter squared. In Ref. [15], the two fixed scales $\mu^2 = Q^2$ and $\mu^2 = s_0^\pi$ were also used in LCSR, as extreme alternatives to the default choice (40). The scale dependence in the region $Q^2 \sim 1 \text{ GeV}^2$ was found rather mild (see Fig. 4 there). Here we only use the scale (40), assuming that it reflects the average virtuality in the correlation function. A more detailed analysis of scale dependence will become possible if in the future

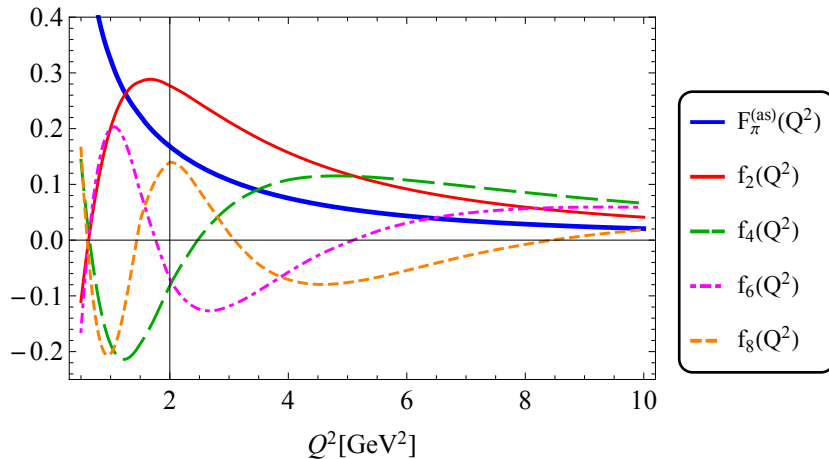


Figure 3: (color online). Separate contributions to Eq. (29) calculated at central values of the input in Table 2 and at the scale (40).

the NNLO effects are taken into account. All other input parameters in LCSR are collected in Table 2.

Parameter	Value	Reference
m_π	139.57 MeV	[43]
f_π	130.4 MeV	[43]
s_0^π	$(0.7 \pm 0.1) \text{ GeV}^2$	[22]
M^2	$(1.2 \pm 0.4) \text{ GeV}^2$	[22]
$\delta_\pi^2(1 \text{ GeV})$	$(0.18 \pm 0.06) \text{ GeV}^2$	[9]
$\langle \bar{q}q \rangle(1 \text{ GeV})$	$-(269_{-4}^{+15})^3 \text{ MeV}^3$	[43]

Table 2: Numerical values of the parameters used in the LCSR (29) for the pion spacelike form factor.

Here we follow the choice in Ref. [22] as far as the effective threshold and the Borel parameter interval are concerned. The two nonperturbative parameters, δ_π^2 and $\langle \bar{q}q \rangle$, enter, respectively, the twist-4 and the factorizable twist-6 terms in Eq. (20). The value of δ_π^2 determining the vacuum-to-pion matrix element (27), is estimated from a dedicated QCD sum rule [9, 45] (see also Ref. [22]). It agrees with the first lattice QCD determination in Ref. [4]. The quark condensate density is obtained from the Gell-Mann-Oakes-Renner relation: $\langle \bar{q}q \rangle = -f_\pi^2 m_\pi^2 / [2(m_u + m_d)]$ taking from Ref. [43] $(m_u + m_d)(2 \text{ GeV}) = 6.9_{-0.3}^{+1.1} \text{ MeV}$. For the quark-gluon coupling we assume the same normalization scale (40) and use the average from Ref. [43]: $\alpha_s(M_Z) = 0.1181 \pm 0.0011$. For the running of α_s and quark masses we employ the RunDec code from Ref. [44] so that e.g. $\alpha_s(1 \text{ GeV}) = 0.486 \pm 0.024$.

To illustrate the interplay of twist-2 contributions to the LCSR (29), in Fig. 3 we plot the form factor $F_\pi^{(\text{as})}(Q^2)$ obtained with the asymptotic DA including the twist-2 NLO as well as the higher-twist contributions. Separately plotted are the coefficient functions $f_n(Q^2, \mu, \mu_0)$ at $n = 2, 4, 6, 8$. We notice that each function f_n vanishes at n values of $Q^2 \geq 0$, due to the zeros of Gegenbauer polynomials.

Having at our disposal the numerical results for both sides of Eq. (39) at multiple values

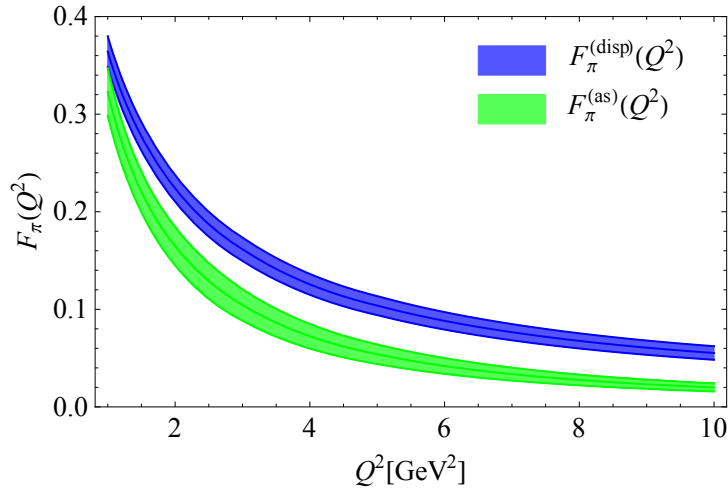


Figure 4: (color online). The pion spacelike form factor calculated from the LCSR with the asymptotic twist-2 pion DA (green band) and from the dispersion relation (11) (blue band) using the timelike form factor specified in Eq. (30).

of Q^2 in the adopted region of validity,

$$1.0 \text{ GeV}^2 \lesssim Q^2 \lesssim 10 \text{ GeV}^2, \quad (41)$$

one may try to form and solve a system of linear equations for the moments a_n . However, this task is not realistic, having in mind a limited accuracy of these equations. Moreover, the LCSR predictions taken at different Q^2 are inevitably correlated.

To proceed, we assume a converging conformal expansion of the DAs, so that

$$a_{n+2}(\mu_0) < a_n(\mu_0), \quad n \geq 0. \quad (42)$$

Under this assumption, it is conceivable to adopt a certain model for the pion twist-2 DA with only $a_2 \neq 0$ or only $a_2, a_4 \neq 0$, etc. After that, using Eq. (39), it is possible to fit the Gegenbauer moments within the adopted model. Moreover, the zeros of f_n provide values of Q^2 at which the contribution of the moment a_n is absent. E.g., as seen from Fig. 3, the coefficient function f_4 at $Q^2 \simeq 2.5 \text{ GeV}^2$ vanishes, enabling one to extract a_2 in a model with the two nonvanishing Gegenbauer moments $a_2, a_4 \neq 0$. Furthermore, since the Q^2 dependence in Eq. (39) is given in an analytical form, one can differentiate over Q^2 both parts of this relation yielding additional constraints.

In this paper, we limit ourselves with an exploratory numerical study of Eq. (39) and only apply a simple fit procedure, assuming that the pion twist-2 DA consists of a certain combination of few first Gegenbauer polynomials.

Before presenting the fit results, let us make the following observation. In Fig. 4, the l.h.s of Eq. (39) calculated assuming the asymptotic twist-2 DA (i.e., at all $a_n = 0$), is compared with the r.h.s. obtained from Eq. (30). An apparent discrepancy clearly indicates that we have to include nonasymptotic terms in the pion twist-2 DA. To this end, we consider four different models of this DA, retaining in the expansion (15) from one to four nonvanishing Gegenbauer moments. For brevity we denote these models as

$$\{a_2\}, \{a_2, a_4\}, \{a_2, a_4, a_6\}, \{a_2, a_4, a_6, a_8\}. \quad (43)$$

For each model we introduce the χ^2 -distribution function:

$$\chi^2 = \sum_{i=1}^{N_p} \frac{1}{\sigma_i^2} \left[\sum_{n=2,4,\dots}^{n_{\max}} a_n(\mu_0) f_n(Q_i^2, \mu_0) + F_\pi^{(\text{as})}(Q_i^2) - F_\pi^{(\text{disp})}(Q_i^2) \right]^2, \quad (44)$$

quantifying the difference between the l.h.s. of Eq. (39) (decomposed according to Eq. (29)) and the r.h.s of the same equation denoted as $F_\pi^{(\text{disp})}(Q_i^2)$. In the sum in Eq. (44), we include $N_p = 7$ "data" points at $Q^2 = \{1.0, 1.5, 2.0, 3.0, 5.0, 7.0, 9.0\}$ GeV² effectively covering the region (41). The weighting coefficients σ_i^2 are calculated according to:

$$\sigma_i = \sqrt{[\Delta F_\pi^{(\text{LCSR})}(Q_i^2, a_n(\mu_0) = 0)]^2 + [\Delta F_\pi^{(\text{disp})}(Q_i^2)]^2}, \quad (45)$$

where the uncertainty $\Delta F_\pi^{(\text{LCSR})}(Q_i^2, a_n(\mu_0) = 0)$ attributed to LCSR at the point Q_i^2 is calculated at vanishing values of the Gegenbauer moments $a_n(\mu_0)$, varying all input parameters within their intervals. The uncertainties due to the coefficient functions f_n are neglected. We have checked that their addition to the weighting coefficients produces numerically insignificant changes in the fit results. The uncertainty $\Delta F_\pi^{(\text{disp})}(Q_i^2)$ of the dispersion relation is estimated, varying the fit parameters quoted in Table 1 within their errors (assumed uncorrelated). We also add to this experiment-induced uncertainty the one due to model-dependence of the high-energy tail in $F_\pi^{(\text{disp})}(Q_i^2)$. The latter uncertainty is estimated, artificially continuing the BaBar fit formula for $F_\pi^{(\text{data})}(s)$ into the region $s > s_{\max}$ and calculating the variation of the dispersion integral caused by this modification. We have found that this variation is limited by $\pm 5\%$.

Minimizing the χ^2 -distribution function (44), we obtain the estimates of the Gegenbauer moments $a_n(\mu_0)$ for all models listed in Eq. (43). Our main numerical results are presented in Table 3 and the corresponding plots are shown in Fig. 5.

Model	$a_2(1 \text{ GeV})$	$a_4(1 \text{ GeV})$	$a_6(1 \text{ GeV})$	$a_8(1 \text{ GeV})$	χ_{\min}^2/ndf
$\{a_2\}$	0.302 ± 0.046				4.08
$\{a_2, a_4\}$	0.279 ± 0.047	0.189 ± 0.060			0.75
$\{a_2, a_4, a_6\}$	0.270 ± 0.047	0.179 ± 0.060	0.123 ± 0.086		0.073
$\{a_2, a_4, a_6, a_8\}$	0.269 ± 0.047	0.185 ± 0.062	0.141 ± 0.096	0.049 ± 0.116	0.013

Table 3: The Gegenbauer moments fitted from Eq. (39) for the models (43) of the pion twist-2 DA. The correlations between the moments are found at the level of $\approx -15\%$.

We emphasize that the fit procedure employed here is an exploratory one, with the aim to demonstrate that the new method of obtaining the pion spacelike form factor works and being combined with LCSR provides constraints on the Gegenbauer moments. In particular, we do not take into account the correlations between "experimental" points in Eq. (44), stemming from the correlations within the data on the timelike form factor. The number of degrees of freedom (ndf) used in the fit is simply equal to the difference of N_p and the number of Gegenbauer moments involved in the model of the pion DA. Increasing N_p does not influence the central values of the fitted Gegenbauer moments but leads to an artificial decrease of χ_{\min}^2/ndf , due to the growth of ndf. The selected N_p is optimal in this respect and, in addition, covers the chosen interval of Q^2 . Further improvement of the statistical

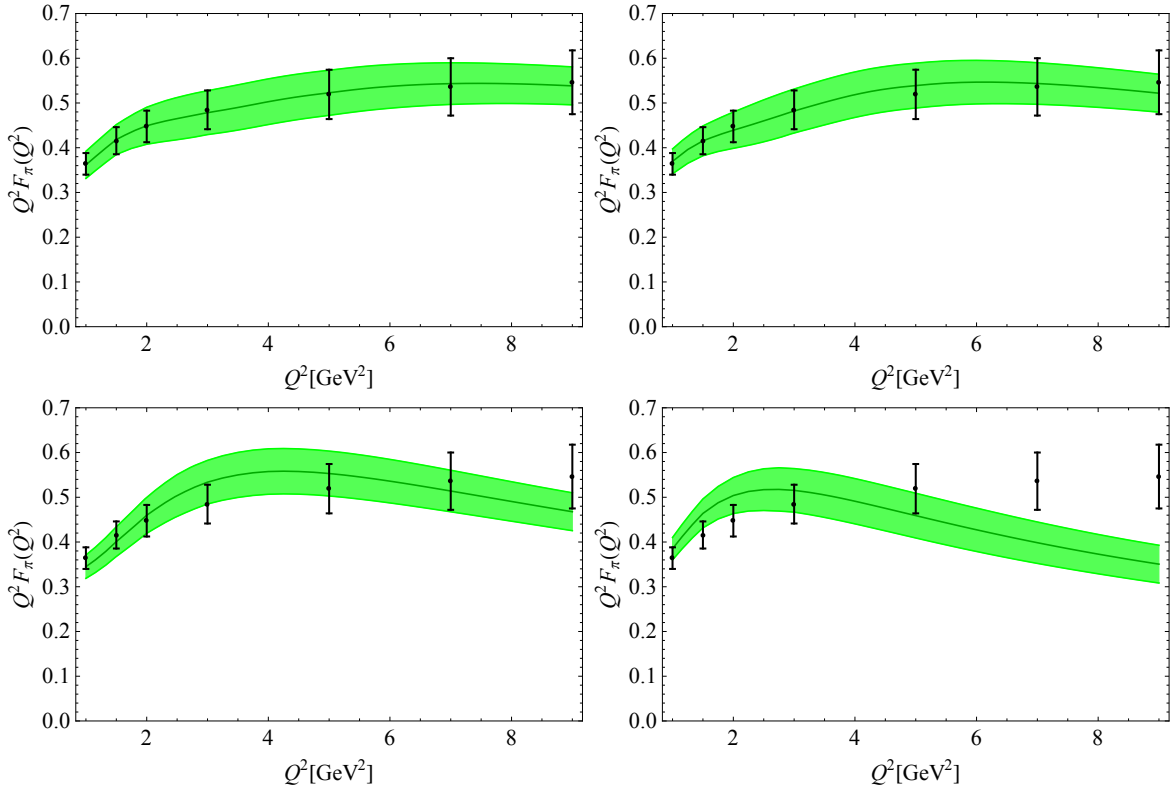


Figure 5: The pion spacelike form factor calculated from the dispersion relation (39) (“data” points with error bars) and from the LCSR with the Gegenbauer moments obtained from the fit (green bands) for the models $\{a_2, a_4, a_6, a_8\}$, $\{a_2, a_4, a_6\}$, $\{a_2, a_4\}$ and $\{a_2\}$, shown, respectively, on the top left, top right, bottom left and bottom right panel.

treatment of the relation (39) is possible provided more detailed data on the timelike form factor become available.

Several comments regarding the results presented in Table 3 are in order:

- The minimal model $\{a_2\}$ with a single Gegenbauer moment is only marginally consistent with Eq. (39). As can be seen from the right bottom plot in Fig. 5, this model does not provide an accurate matching between the LCSR and dispersion relation at all Q^2 .
- The simplest non-minimal model $\{a_2, a_4\}$ yields a satisfactory fit which becomes even better for the models $\{a_2, a_4, a_6\}$ and $\{a_2, a_4, a_6, a_8\}$.
- The fitted value of a_8 in the model $\{a_2, a_4, a_6, a_8\}$ is consistent with zero within uncertainties. In addition, we have probed models containing moments with $n > 8$ and found that this tendency persists: the fit returns small coefficients $a_{n \geq 8}$ with large errors, retaining practically similar ranges of the first three Gegenbauer moments. The main reason is a strong and sign alternating oscillation of the coefficient functions f_n at large n .
- Generally, the fitted pattern of Gegenbauer moments is in accordance with a convergent conformal expansion (42).

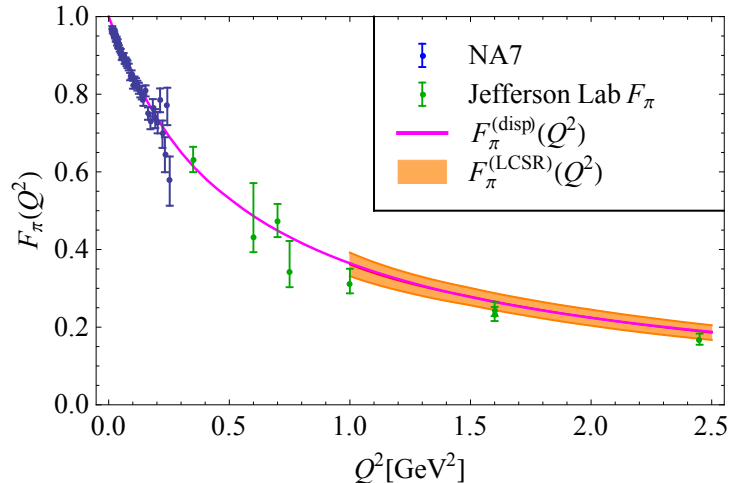


Figure 6: (color online). The pion spacelike form factor calculated from the dispersion relation (39) (magenta curve; central input) and from the LCSR with the fitted Gegenbauer moments (orange band; the model $\{a_2, a_4, a_6, a_8\}$) compared with the measurements of NA7 [24] (blue data points) and Jefferson Lab F_π [20] (green data points).

- As can be seen from Table 3, for all three non-minimal models that we consider, the fitted values of the second and fourth Gegenbauer moment cover approximately the same intervals:

$$a_2(1 \text{ GeV}) = 0.22 - 0.33, \quad a_4(1 \text{ GeV}) = 0.12 - 0.25. \quad (46)$$

We refrain from quoting central values and standard deviations instead of these intervals, having in mind limitations of our statistical analysis.

It is instructive to compare our results with the pion spacelike form factor measurements not used in the fit. This comparison is displayed in Fig. 6 where the two (correlated) results: the spacelike form factor obtained from the dispersion relation at $Q^2 = -q^2 \geq 0$ and from LCSR in the region (41) with the fitted Gegenbauer moments (the model $\{a_2, a_4, a_6, a_8\}$), are plotted together with the Jefferson Lab F_π data [20] at intermediate Q^2 and the NA7 data [24] at very small Q^2 . We observe an agreement within uncertainties and experimental errors, whereas at $Q^2 > 1.0 \text{ GeV}^2$ the central values of the predicted form factor lie slightly above the experimental points.

Furthermore, having at our disposal the modulus of the pion form factor at sufficiently large timelike momentum transfer $\sqrt{s} = \sqrt{|q^2|}$, we compare it with the form factor at large spacelike $\sqrt{Q^2} = \sqrt{|q^2|}$ inferred from Eq. (11). In Fig. 7 the overlap of the two form factors at equal values of $\sqrt{|q^2|}$ is plotted. Note that this comparison does not involve any LCSR results. At $\sqrt{|q^2|} \gtrsim 3.0 \text{ GeV}$, above the region of pronounced resonances, we observe an onset of a regime in which the timelike form factor approximately coincides with the spacelike one. Generally, this equality manifests analyticity of the modulus representation. At the same time, since the form factor at large Q^2 is well reproduced by the LCSR based on a quark-gluon correlation function (cf. the comparison in Fig. 6), it is conceivable to interpret this coincidence as the onset of the quark-hadron duality: calculating the form factor at a sufficiently large Q^2 in terms of the quark-gluon degrees of freedom, we are able to predict the timelike pion form factor at $s = Q^2$. Note on the other hand that in this

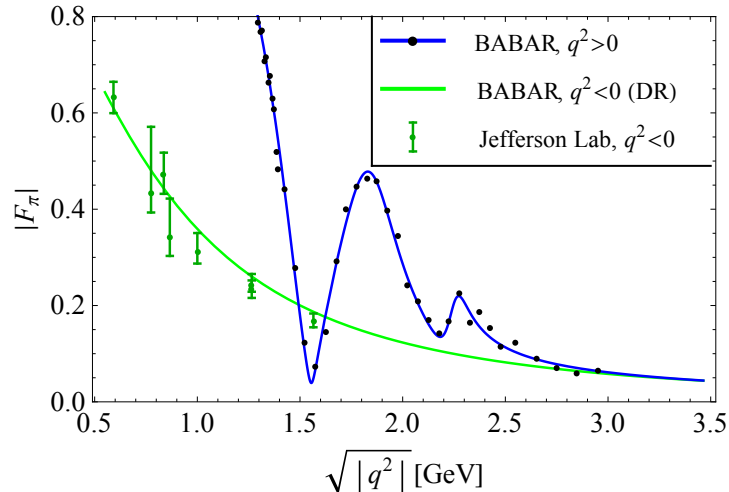


Figure 7: (color online). The pion timelike form factor measured by the BaBar collaboration [25] (black points (the central values) and the fit (blue curve)) and the pion spacelike form factor obtained from the dispersion relation (11) (green curve). The Jlab data are shown by green points with error bars.

region the form factor is still far from QCD asymptotics and, as follows e.g. from LCSR, is dominated by soft overlap contributions. To see that, we use the well known asymptotic formula [27–30]:

$$\lim_{Q^2 \rightarrow \infty} F_\pi(Q^2) = \frac{8\pi\alpha_s}{9Q^2} f_\pi^2 \left(\int_0^1 \frac{du}{u} \varphi_\pi(u, \mu) \right)^2, \quad (47)$$

(cf. Eq. (25)). Adopting for the pion DA, e.g., the model $\{a_2, a_4, a_6\}$ with Gegenbauer moments from Table 3 and the characteristic scale $\mu \sim \sqrt{Q^2}$, we obtain that in the ballpark of the “duality” region, at $Q^2 = 10 \text{ GeV}^2$, the r.h.s. of the above equation is equal to $\simeq 0.019$, substantially smaller than the value $F_\pi^{(\text{disp})}(Q^2 = 10 \text{ GeV}^2) \simeq 0.05$ predicted by the dispersion relation.

Let us compare our estimates of Gegenbauer moments with the results of other methods. A useful compilation can be found in Ref. [1] (see Table 4 there). We start from the determinations of a_2 that are independent of the experimental data and not correlated with higher moments. First of all, the moment a_2 is accessible in the lattice QCD. The most accurate value has been recently obtained in Ref. [1]. Rescaling it to the default scale:

$$a_2(1 \text{ GeV}) = 0.135 \pm 0.032, \quad (48)$$

we find that our fitted values in Table 3 and in Eq. (46) are noticeably larger. Fixing a_2 from the lattice QCD result (48), we have repeated the fit of Eq. (39). The results are given in Table 4 (see also Fig. 8) for the three models $\{a_2, a_4\}$, $\{a_2, a_4, a_6\}$, $\{a_2, a_4, a_6, a_8\}$. We notice that the values of a_4, a_6 increase and the quality of the fit becomes worse in comparison with our initial results in Table 3.

Another method [7] to calculate a_2 is based on the QCD sum rules for a two-point vacuum correlation function. Comparing our results with the estimate $a_2(1 \text{ GeV}) = 0.28 \pm 0.08$ obtained by this method in Ref. [9] (see also Ref. [8]) we observe a good agreement.

The Gegenbauer moments with $n > 2$ were obtained from the QCD sum rules with nonlocal condensates, predicting $a_2(1 \text{ GeV}) \simeq 0.20$, $a_4(1 \text{ GeV}) \simeq -0.14$ [11, 18]. A striking

Model	$a_4(1 \text{ GeV})$	$a_6(1 \text{ GeV})$	$a_8(1 \text{ GeV})$	χ^2_{\min}/ndf
$\{a_2, a_4\}$	0.218 ± 0.059			3.93
$\{a_2, a_4, a_6\}$	0.203 ± 0.060	0.157 ± 0.086		2.81
$\{a_2, a_4, a_6, a_8\}$	0.210 ± 0.061	0.179 ± 0.095	0.062 ± 0.116	2.71

Table 4: The same as in Table 3 but with a fixed value of a_2 from Eq. (48).

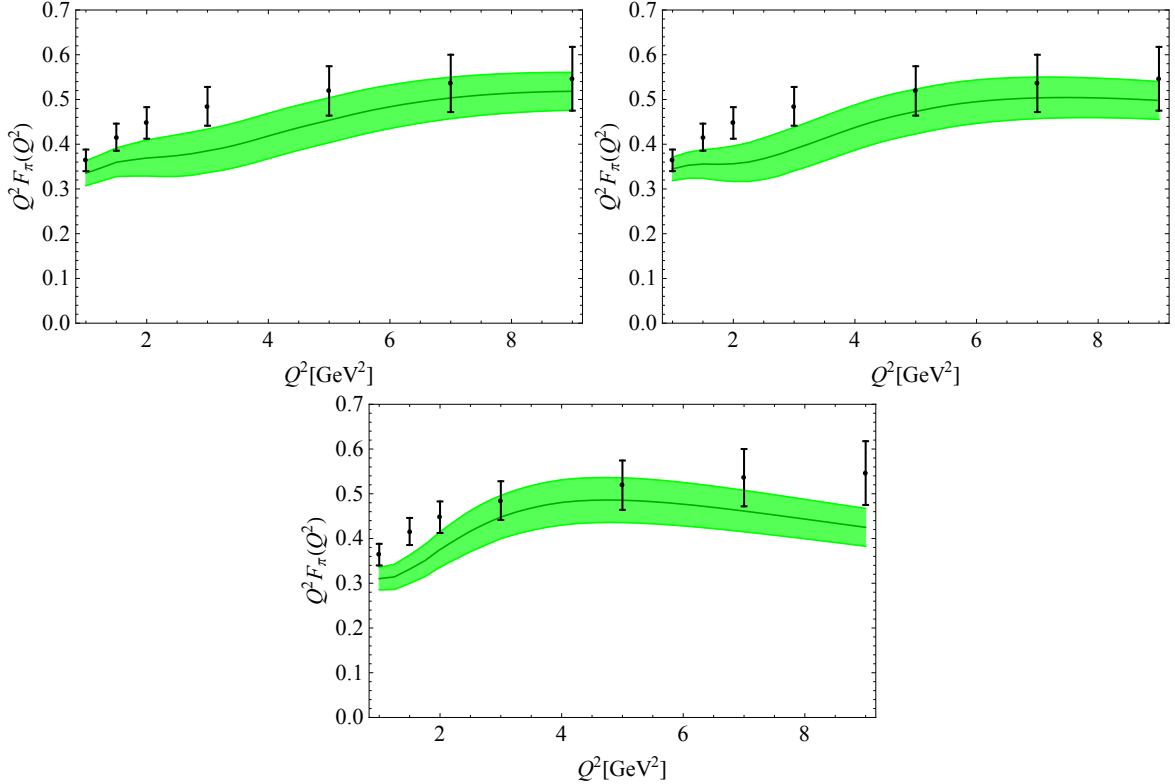


Figure 8: The same as in Fig. 5 but with a fixed value of a_2 from Eq. (48). The results for the models $\{a_2, a_4, a_6, a_8\}$, $\{a_2, a_4, a_6\}$, and $\{a_2, a_4\}$ are shown, respectively, on the top left, top right, and bottom panel.

difference with respect to our estimates is the negative sign of the fourth Gegenbauer moment. The first lattice QCD values of a_4 obtained with the new method of Euclidean correlation function in Ref. [4] still have very large uncertainties.

A different strategy is to match an analytical expression for the pion e.m. form factor in terms of twist-2 DA to the measured values in the spacelike region. Certainly, the use of a hard-scattering factorization formula e.g., of the asymptotic expression in Eq. (47) is not an adequate choice, because, as we have convinced ourselves, at large but finite Q^2 the soft overlap part of the form factor dominates. Instead, in several analyses, the LCSR written in the form of Eq. (29) was employed. As opposed to the method we suggest here, this equation was directly fitted to the measured form factor. E.g., in Ref. [21], the LCSR with the model $\{a_2, a_4\}$ was fitted to the Jefferson Lab F_π data [20] in the region $0.6 \text{ GeV}^2 < Q^2 < 2.45 \text{ GeV}^2$. The results

$$a_2(1 \text{ GeV}) = 0.17 \pm 0.08, \quad a_4(1 \text{ GeV}) = 0.06 \pm 0.10$$

have larger uncertainties than our fit results for the same model in Table 3 and marginally

agree with the latter within errors. Certainly, the use of a dispersion relation has an advantage of giving access to a considerably larger region of the spacelike momentum transfer.

Method	$a_2(1 \text{ GeV})$	$a_4(1 \text{ GeV})$	Ref.
Lattice QCD	0.135 ± 0.032	–	[1]
QCD sum rule	0.28 ± 0.08	–	[9]
QCD sum rule with nonlocal condensate	$0.203^{+0.069}_{-0.057}$	$-0.143^{+0.094}_{-0.087}$	[18, 19]
LCSR fitted to Jlab data	0.17 ± 0.08	0.06 ± 0.10	[21]
LCSR fitted to dispersion relation	0.22 - 0.33	0.12 - 0.25	this work

Table 5: Comparison of the second and fourth Gegenbauer moments obtained with various methods.

For convenience, in Table 5 we put together the results on a_2 and a_4 obtained with various methods and discussed above. The most important findings which deserve further attention and investigations are: 1) our estimated interval for a_2 lies above the lattice QCD prediction, and probably also above the result from the LCSR fitted to the Jlab data; 2) the LCSR fits prefer a positive sign of a_4 , opposite to the one predicted from the sum rules with nonlocal condensates.

Gegenbauer moments are also constrained from the photon-pion transition form factor measured in the $\gamma^*\gamma \rightarrow \pi^0$ process. To calculate this form factor, one uses the method of Ref. [16], combining a dispersion relation in the photon virtuality with LCSR. The accuracy of this method was improved in Ref. [17] calculating important additional terms in the LCSR. A more recent analysis of $\gamma^*\gamma \rightarrow \pi^0$ with related methods can be found in Ref. [46]. The main problem of using the photon-pion transition form factor is a mutual discrepancy between the results of different experiments, especially at large Q^2 . We postpone a more detailed discussion and only mention, for comparison, the model $\{a_2, a_4, a_6, a_8\}$ used to fit the data in Ref. [17] (the model II):

$$\begin{aligned} a_2(1 \text{ GeV}) &= 0.10 - 0.14, & a_4(1 \text{ GeV}) &= 0.10 - 0.18, \\ a_6(1 \text{ GeV}) &= 0.10 - 0.23, & a_8(1 \text{ GeV}) &= 0.034 - 0.05, \end{aligned}$$

where the upper and lower limits correspond to different experiments. This model has the same sign pattern as our fit results but has a smaller second moment and does not reveal a convergent conformal expansion.

6 Conclusion

In this paper we suggested a new method to probe the twist-2 pion DA by comparing two independent ways to calculate the pion e.m. form factor in the spacelike region. The first one employs the modified dispersion relation (modulus representation) in which the input is essentially provided by the direct measurement of the pion e.m. form factor in the timelike region. The same form factor is calculated from the LCSR with a linear dependence on the Gegenbauer moments taken at a certain reference normalization scale. We performed an exploratory numerical investigation of the equation between LCSR and dispersion relation, employing for the latter the BaBar collaboration data on the pion timelike form factor.

Adopting simple models of the pion DA, we fitted the first few Gegenbauer moments. This analysis reveals certain gross features of the pion DA: its form deviates from the purely asymptotic one; the minimal ansatz with a single Gegenbauer moment a_2 is disfavoured and the validity of a converging conformal expansion is confirmed. Our main results are given in Table 3 and yield intervals (46) for the second and fourth moments. Numerically, our prediction for a_2 is in the same ballpark as the two-point QCD sum rule estimates, but exceeds the currently most accurate lattice QCD value. We also found that the spacelike form factor extracted from the dispersion relation is consistent within errors with the Jlab data. Importantly, this form factor at large momentum transfers $Q^2 \sim 10 \text{ GeV}^2$ is still considerably larger than its perturbative QCD asymptotics. This is in accordance with the first lattice QCD calculations [47, 48] of the light meson form factors at large spacelike momentum transfers.

Turning to future perspectives of the method suggested in this paper, let us first of all mention possible modifications of the specific dispersion relation (modulus representation) used here. In particular, the role of form factor zeros should be investigated. Additional subtractions and/or differentiation in Q^2 can provide an effective suppression of the high-energy tail of the timelike form factor which is not directly measured. The fit procedure applied in this paper can further be extended to include the data on the direct measurements of the spacelike form factor. In the timelike region, one may additionally employ the pion vector form factor measured in $\tau^- \rightarrow \pi^- \pi^0 \nu_\tau$ decays. Eventually, our analysis should be complemented with the fit of the measured photon-pion form factor for which the LCSR-based theoretical expression contains the same input as the one used for the pion e.m. form factor.

Needless to say, the accuracy of the fit will benefit from new more accurate data on all types of the pion form factor. Note that both the region of large Q^2 for the photon-pion form factor and the region of large s for the pion timelike e.m. and vector form factors are potentially accessible at Belle II. Finally, we foresee a perspective application of the same method to the kaon DA, employing the kaon e.m. form factor as well as the flavour-changing form factors in $\tau \rightarrow K \pi \ell \nu_\ell$ decays.

Acknowledgements

We are grateful to Irinel Caprini for useful comments. A.K. and A.R. would like to thank the Mainz Institute for Theoretical Physics (MITP) of the Cluster of Excellence PRISMA+ (Project ID 39083149) for hospitality and support. S.C. is supported by the National Science Foundation of China (NSFC) under Grant No. 11805060 and the Natural Science Foundation of Hunan Province, China (Grant No.2020JJ4160). The work of A.K. is supported by the Deutsche Forschungsgemeinschaft (German Research Foundation) under grant 396021762 - TRR 257. A.R. acknowledges support by the STFC grant of the IPPP.

Appendix

Here we present the expression for the Gounaris-Sakurai resonance formula used in Eq. (31):

$$\text{BW}_R^{\text{GS}}(s) = \frac{m_R^2 + m_R \Gamma_R d(m_R)}{m_R^2 - s + f(s, m_R, \Gamma_R) - i m_R \Gamma(s, m_R, \Gamma_R)}, \quad (49)$$

where $R = \rho, \rho', \rho'', \rho'''$ and the functions entering this expression are

$$\begin{aligned}
\Gamma(s, m, \Gamma) &= \Gamma \frac{s}{m^2} \left(\frac{\beta_\pi(s)}{\beta_\pi(m^2)} \right)^3, & \beta_\pi(s) &= \sqrt{1 - 4m_\pi^2/s}, \\
d(m) &= \frac{3}{\pi} \frac{m_\pi^2}{k^2(m^2)} \ln \left(\frac{m + 2k(m^2)}{2m_\pi} \right) + \frac{m}{2\pi k(m^2)} - \frac{m_\pi^2 m}{\pi k^3(m^2)}, \\
f(s, m, \Gamma) &= \frac{\Gamma m^2}{k^3(m^2)} (k^2(s)(h(s) - h(m^2)) + (m^2 - s)k^2(m^2)h'(m^2)), \\
k(s) &= \frac{1}{2} \sqrt{s} \beta_\pi(s), \\
h(s) &= \frac{2}{\pi} \frac{k(s)}{\sqrt{s}} \ln \left(\frac{\sqrt{s} + 2k(s)}{2m_\pi} \right), & h'(s) &= \frac{dh(s)}{ds}.
\end{aligned}$$

and the KS representation used for the ω -resonance is given by

$$\text{BW}_\omega^{\text{KS}}(s, m_\omega, \Gamma_\omega) = \frac{m_\omega^2}{m_\omega^2 - s - i m_\omega \Gamma_\omega}. \quad (50)$$

References

- [1] G. S. Bali, V. M. Braun, S. Bürger, M. Göckeler, M. Gruber, F. Hutzler, P. Korcyl, A. Schäfer, A. Sternbeck and P. Wein, *JHEP* **08** (2019), 065.
- [2] R. Arthur, P. Boyle, D. Brommel, M. Donnellan, J. Flynn, A. Juttner, T. Rae and C. Sachrajda, *Phys. Rev. D* **83** (2011), 074505.
- [3] V. M. Braun, S. Collins, M. Göckeler, P. Pérez-Rubio, A. Schäfer, R. W. Schiel and A. Sternbeck, *Phys. Rev. D* **92** (2015) no.1, 014504.
- [4] G. S. Bali, V. M. Braun, B. Gläble, M. Göckeler, M. Gruber, F. Hutzler, P. Korcyl, B. Lang, A. Schäfer, P. Wein and J. Zhang, *Eur. Phys. J. C* **78** (2018) no.3, 217; *Phys. Rev. D* **98** (2018) no.9, 094507.
- [5] R. Zhang, C. Honkala, H. W. Lin and J. W. Chen [arXiv:2005.13955 [hep-lat]].
- [6] M. A. Shifman, A. Vainshtein and V. I. Zakharov, *Nucl. Phys. B* **147** (1979), 385-447.
- [7] V. Chernyak and A. Zhitnitsky, *Nucl. Phys. B* **201** (1982), 492; *Phys. Rept.* **112** (1984), 173.
- [8] A. Khodjamirian, T. Mannel and M. Melcher, *Phys. Rev. D* **70** (2004), 094002.
- [9] P. Ball, V. Braun and A. Lenz, *JHEP* **05** (2006), 004.
- [10] S. Mikhailov and A. Radyushkin, *JETP Lett.* **43** (1986), 712.
- [11] A. P. Bakulev, S. V. Mikhailov and N. G. Stefanis, *Phys. Lett. B* **508** (2001), 279-289.
- [12] I. Balitsky, V. M. Braun and A. Kolesnichenko, *Sov. J. Nucl. Phys.* **44** (1986), 1028; *Nucl. Phys. B* **312** (1989), 509-550.

- [13] V. Chernyak and I. Zhitnitsky, Nucl. Phys. B **345** (1990), 137-172 .
- [14] V. M. Braun and I. E. Halperin, Phys. Lett. B **328** (1994), 457-465 .
- [15] V. M. Braun, A. Khodjamirian and M. Maul, Phys. Rev. D **61** (2000), 073004 .
- [16] A. Khodjamirian, Eur. Phys. J. C **6** (1999), 477-484 .
- [17] S. Agaev, V. Braun, N. Offen and F. Porkert, Phys. Rev. D **83** (2011), 054020; Phys. Rev. D **86** (2012), 077504 .
- [18] S. Mikhailov, A. Pimikov and N. Stefanis, Phys. Rev. D **93** (2016) no.11, 114018 .
- [19] N. G. Stefanis, Phys. Rev. D **102** (2020) no.3, 034022 .
- [20] G. Huber *et al.* [Jefferson Lab], Phys. Rev. C **78** (2008), 045203 .
- [21] A. Khodjamirian, T. Mannel, N. Offen and Y. Wang, Phys. Rev. D **83** (2011), 09403 .
- [22] J. Bijnens and A. Khodjamirian, Eur. Phys. J. C **26** (2002), 67-79 .
- [23] S. Agaev, Phys. Rev. D **72** (2005), 074020 .
- [24] S. Amendolia *et al.* [NA7], Nucl. Phys. B **277** (1986), 168 .
- [25] J. Lees *et al.* [BaBar], Phys. Rev. D **86** (2012), 032013 .
- [26] M. Fujikawa *et al.* [Belle], Phys. Rev. D **78** (2008), 072006 .
- [27] V. Chernyak, A. Zhitnitsky and V. Serbo, JETP Lett. **26** (1977), 594-597 .
- [28] G. R. Farrar and D. R. Jackson, Phys. Rev. Lett. **43** (1979), 246 .
- [29] A. Efremov and A. Radyushkin, Phys. Lett. B **94** (1980), 245-250 .
- [30] G. Lepage and S. J. Brodsky, Phys. Rev. D **22** (1980), 2157 .
- [31] A. Pich and J. Portoles, Phys. Rev. D **63** (2001), 093005 .
- [32] C. Hanhart, Phys. Lett. B **715** (2012), 170-17 .
- [33] N. Achasov and A. Kozhevnikov, Phys. Rev. D **83** (2011), 113005 .
- [34] G. Colangelo, M. Hoferichter and P. Stoffer, JHEP **02** (2019), 006 .
- [35] B. Geshkenbein, Yad. Fiz. **9** (1969), 1232-1235; Phys. Rev. D **61** (2000), 033009 .
- [36] H. Leutwyler, [arXiv:hep-ph/0212324 [hep-ph]]. In Proc. "Continuous advances in QCD. Minneapolis, USA (2002)" .
- [37] B. Ananthanarayan, I. Caprini and I. Imsong, Phys. Rev. D **83** (2011), 096002 .
- [38] B. Ananthanarayan, I. Caprini and I. Imsong, Phys. Rev. D **85** (2012), 096006 .
- [39] C. Dominguez, Phys. Lett. B **512** (2001), 331-334 .

- [40] C. Bruch, A. Khodjamirian and J. H. Kühn, Eur. Phys. J. C **39** (2005), 41-54.
- [41] G. Gounaris and J. Sakurai, Phys. Rev. Lett. **21** (1968), 244-247.
- [42] J. H. Kühn and A. Santamaria, Z. Phys. C **48** (1990), 445-452.
- [43] M. Tanabashi *et al.* [Particle Data Group], Phys. Rev. D **98** (2018) no.3, 030001, and 2020 update.
- [44] K. Chetyrkin, J. H. Kühn and M. Steinhauser, Comput. Phys. Commun. **133**, 43-65 (2000) [arXiv:hep-ph/0004189 [hep-ph]].
- [45] V. Novikov, M. A. Shifman, A. Vainshtein, M. Voloshin and V. I. Zakharov, Nucl. Phys. B **237** (1984), 525-552.
- [46] Y. M. Wang and Y. L. Shen, JHEP **12** (2017), 037.
- [47] J. Koponen, A. C. Zimmermann-Santos, C. T. H. Davies, G. P. Lepage and A. T. Lytle, Phys. Rev. D **96** (2017) no.5, 054501.
- [48] A. J. Chambers *et al.* [QCDSF, UKQCD and CSSM], Phys. Rev. D **96** (2017) no.11, 114509.